[Journal of the Faculty of Science, Hokkaidô University, Japan, Ser. VII, Vol. I, No. 3, 1959]

LOVE-waves in Stratified Three Layers

(Continued)

Hiroshi OKADA and Kyozi TAZIME

(Received Octover 22, 1959)

Abstract

At first, some examples are calculated of the dispersion curve, the amplitude function and the amplitude distribution for the first order of LOVE-waves. These calculations remained for cases (A) and (B) in eq. (57) in the previous paper[6].

Next, for cases (C) and (D) in eq. (57), the other examples for the zeroth and the first orders of LOVE-waves are presented.

Lastly, some physical considerations as to these calculations are given.

13. Numerical calculations of the dispersion curve for L_1 in cases (A) and (B)

The dispersion curve for the zeroth order of LOVE-waves, noted by L_0, were already calculated for cases (A) and (B) of (57) in Sec. 9. The rigidity ratios adopted in the numerical calculation were (a) $\mu_2/\mu_1=4$ and $\mu_3/\mu_2=30$, (b) $\mu_2/\mu_1=30$ and $\mu_3/\mu_2=30$, (c) $\mu_2/\mu_1=1/16$ and $\mu_3/\mu_2=30$ and (d) $\mu_2/\mu_1=1/3$ and $\mu_3/\mu_2=30$.

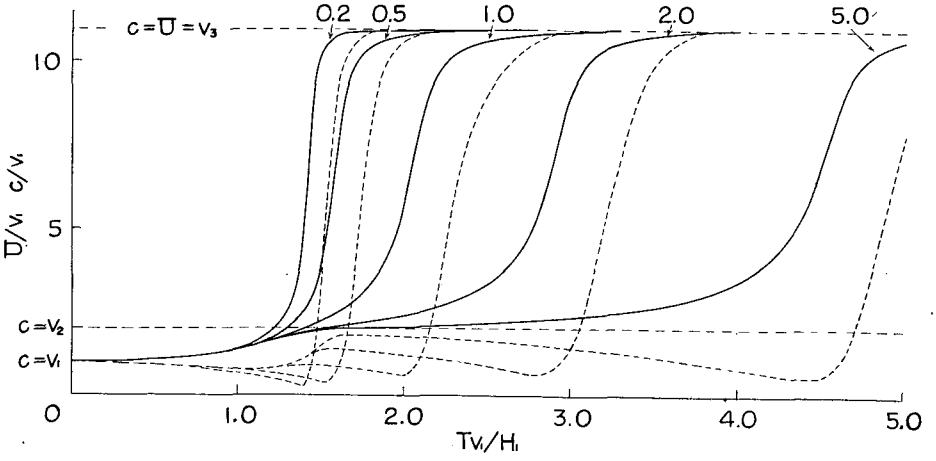

Fig. 7 (a). L_1

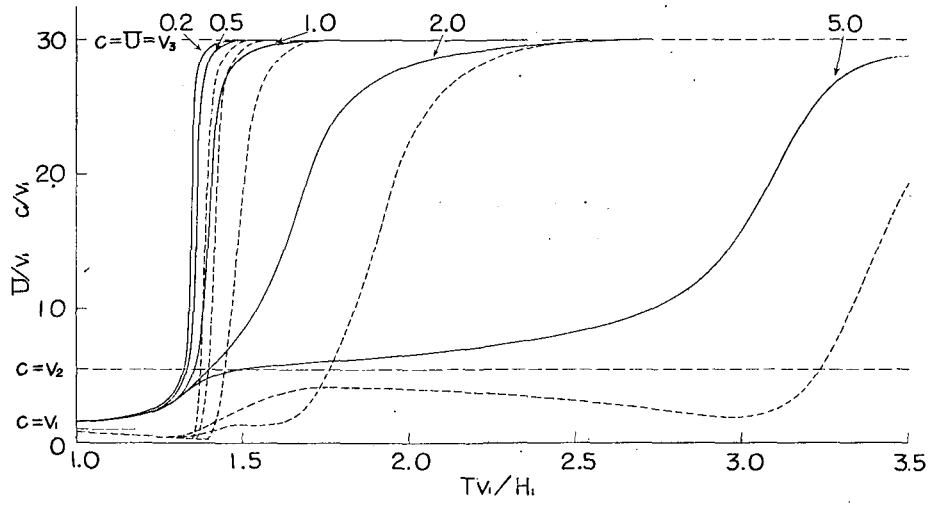

Fig. 7 (b). $\mathbf{L}_1$

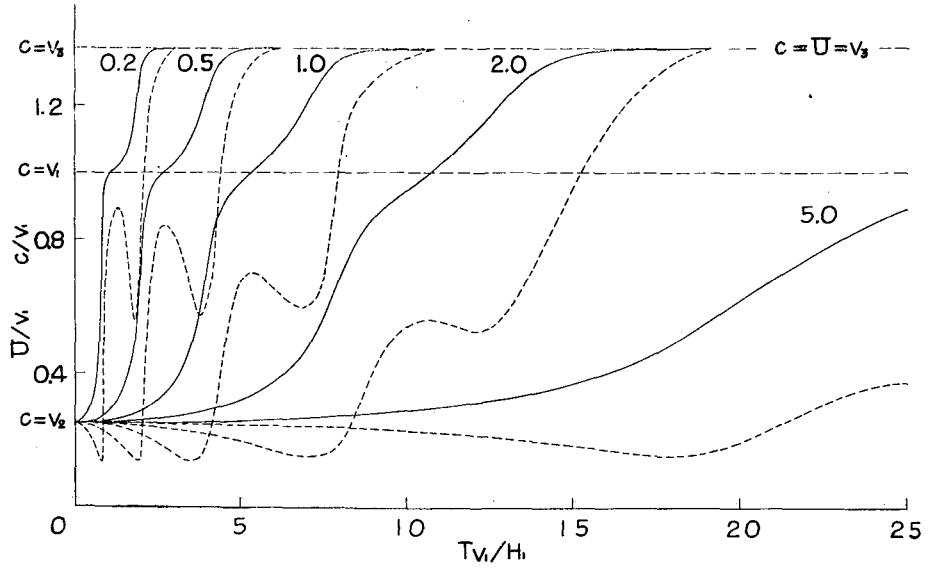

Fig. 7 (c). $\mathbf{L}_1$

The dispersion curve for the first order of LOVE-waves, noted by $\mathbf{L}_1$, has been calculated in this section, adopting the same rigidity ratios as before. The results are shown in Figs. 7(a) to 7(d) for various values of the parameter

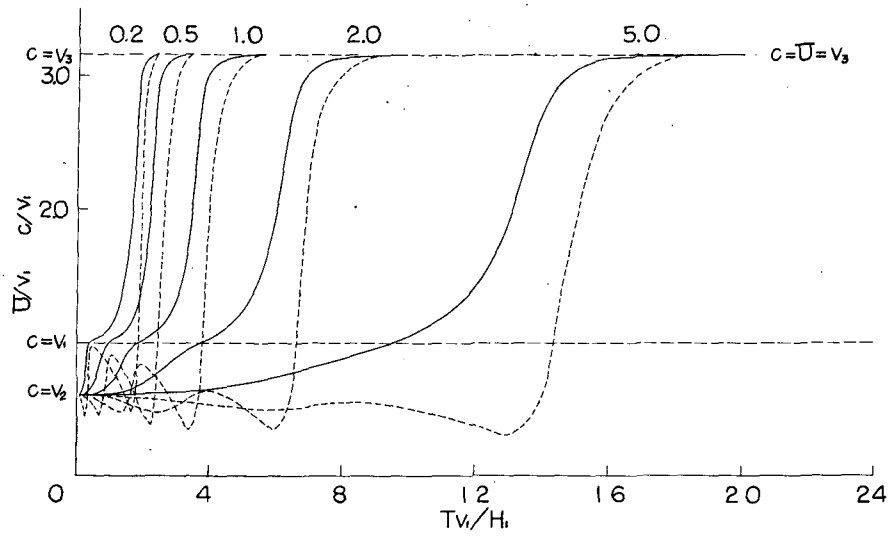

Fig. 7 (d). $\mathbf{L}_1$

Fig. 7. Dispersion curves for $\mathbf{L}_1$ in cases (A) and (B).
(a) $\mu_2/\mu_1 = 4$ and $\mu_3/\mu_2 = 30$, (b) $\mu_2/\mu_1 = 30$ and $\mu_3/\mu_2 = 30$
(c) $\mu_2/\mu_1 = 1/16$ and $\mu_3/\mu_2 = 30$, (d) $\mu_2/\mu_1 = 1/3$ and $\mu_3/\mu_2 = 30$

H_2/H_1.

Whereas $\mathbf{L}_0$ has no cutoff period, $\mathbf{L}_1$ has a finite cutoff period at which phase- and group-velocities must coincide with the velocity of S-wave in the lowest layer. Periods of $\mathbf{L}_1$ must be confined between the cutoff and zero.

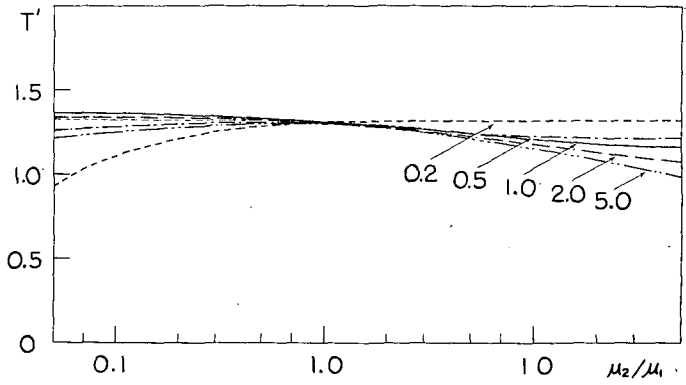

Fig. 8. The period corresponding to the second minimum group velocity for $\mathbf{L}_1$ in cases (A) and (B). $T' = T/(H_1/v_1 + H_2/v_2)$.

Group velocity has two minima as in the case of the zeroth order; one is near $T/(H_1/v_1) = 4/3$ and another is near $T/(H_1/v_1+H_2/v_2)=4/3$, for the rigidity ratios (a) and (b). The latter relation will be clear from Fig. 8 where μ_3/μ_2 is kept at 30.

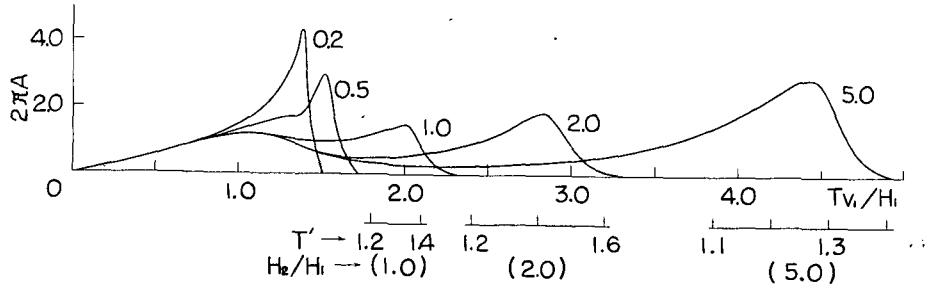

Fig. 9 (a). $\mathbf{L}_1$

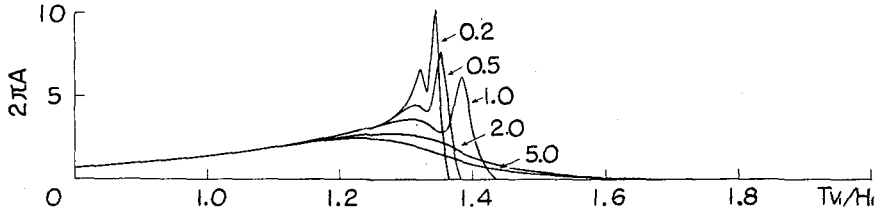

Fig. 9 (b). $\mathbf{L}_1$

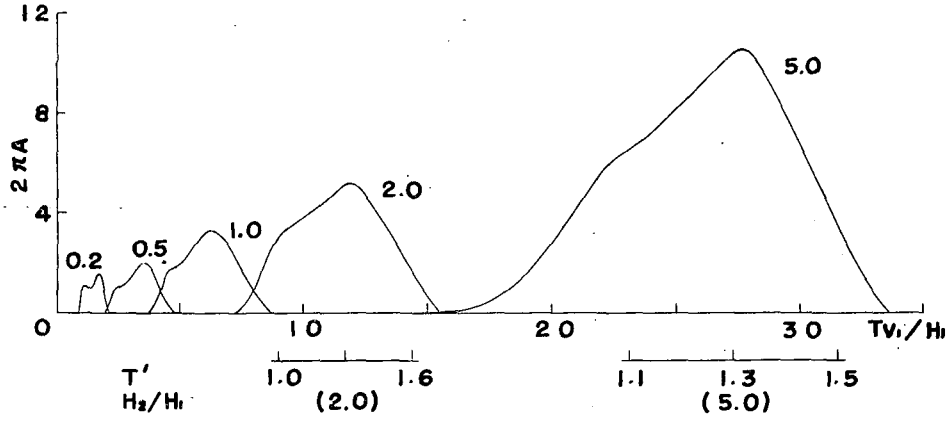

Fig. 9 (c). $\mathbf{L}_1$

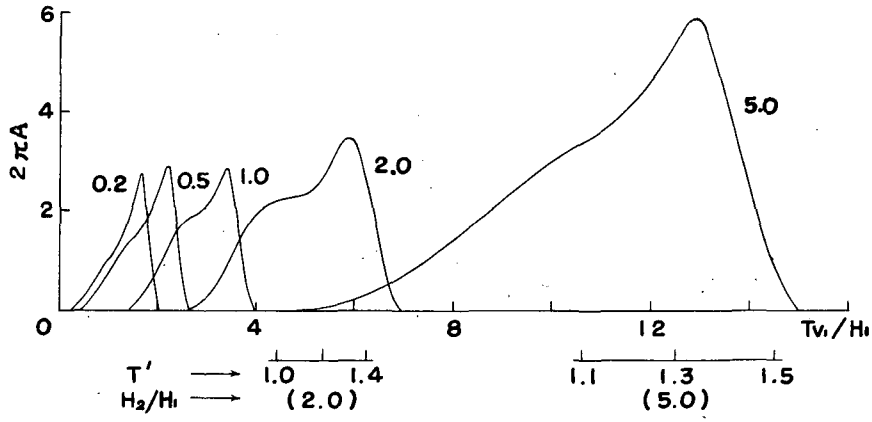

Fig. 9 (d). $\mathbf{L}_1$

Fig. 9. Amplitude functions for $\mathbf{L}_1$ in cases (A) and (B).
$T' = T/(H_1/v_1+H_2/v_2)$.

14. Numerical calculations of the amplitude fuuction for $\mathbf{L}_1$ in cases (A) and (B)

The amplitude function $2\pi A(\xi)$ in (45) has been obtained by using the dispersion curve illustrated in Fig. 7. The results are shown in Figs. 9 (a) to 9 (d) as functions of period Tv_1/H_1.

These amplitude functions may have two maxima in each case. It must be noticed that the first maximum in cases (c) and (d) occurs respectively near the period of the maximum group velocity, whereas the other maxima,

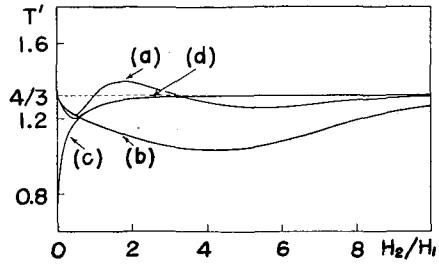

Fig. 10. The period corresponding to the second maximum of the amplitude function for $\mathbf{L}_1$ in cases (A) and (B).
$T'=T/(H_1/v_1+H_2/v_2)$.
(a) : (4, 30), (b) : (30, 30), (c) : (1/16, 30), (d) : (1/3, 30)

the first maximum in cases (a) and (b) and the second maximum in all cases, occur respectively near the period of the minimum group velocity.

Fig. 10 shows the relation between the period of the second maximum of the amplitude function and H_2/H_1, being parameters $(\mu_2/\mu_1,\ \mu_3/\mu_2)$. It is clear that each curve will approach to the period indicated by $T/(H_1/v_1+H_2/v_2)=4/3$ with the increase of H_2/H_1.

Now it has been found that either $\mathbf{L}_0$ or $\mathbf{L}_1$ must obey the wave-length law in general,

$$T/(H_1/v_1) \text{ or } T/(H_1/v_1+H_2/v_2)=4/(2n+1)\,, \quad \begin{pmatrix} n=0 \text{ for } \mathbf{L}_0 \\ =1 \text{ for } \mathbf{L}_1 \end{pmatrix} \qquad (64)$$

at least qualitatively. The thickness of the layers may have larger influence on $\mathbf{L}_1$ than on $\mathbf{L}_0$, because the former has shorter wave-length than the latter. Comparing Fig. 10 with Fig. 5, the asymptotic value of (64) seems to be easily attained by $\mathbf{L}_1$ rather than by $\mathbf{L}_0$. But the ratios of deviation from the asymptotic value are nearly equal to each other for the same value of H_2/H_1.

This situation may also be seen in the relation between the sharpness of the maximum of the amplitude function and the period. The higher the order of the waves, the narrower the band of the period having considerably large amplitude.

It will be physically expected that the amplitude function may arrive at the maximum near the period of the mimimum group velocity. Analytically, this phenomenon may be easily recognized by the factor $(v_1/U-v_1/c)$ in (45). On the other hand, it will seem strange that the amplitude function may arrive at the first maximum near the period of the maximum group velocity in cases (c) and (d). Numerically, the present authors have found that the factor $\{1-(v_1/c)^2\}^{-1}$ in (45) plays the greatest role in these cases.

The latter phenomenon must be accompanied by the "low velocity layer". Considerable energies will escape from the most superficial layer to the low velocity one. Thus the wave of short length cannot keep the law of (64), but ignores that law. Displacement of the wave of short length has the factor $\cosh \hat{\eta}_1 z$ as shown in (iii) of page 126. If c coincides with v_1, $\cosh \hat{\eta}_1 z$ becomes unity for each depth, resulting in large displacement on the surface of the earth for a certain amplitude on the lower boundary of the most superficial layer.

15. Numerical calculations of the amplitude distribution for $\mathbf{L}_1$ in cases (A) and (B)

Figs. 11(a) to 11(d) illustrate the results calculated for several periods

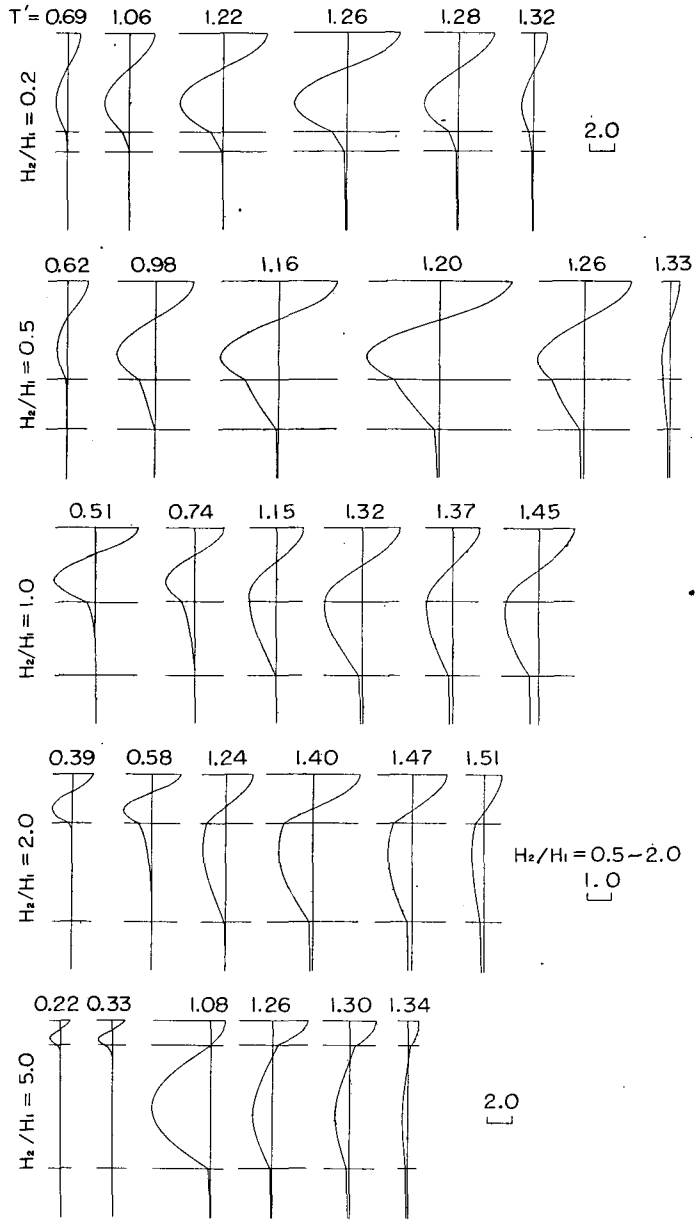

Fig. 11 (a). $\mathbf{L_1}$

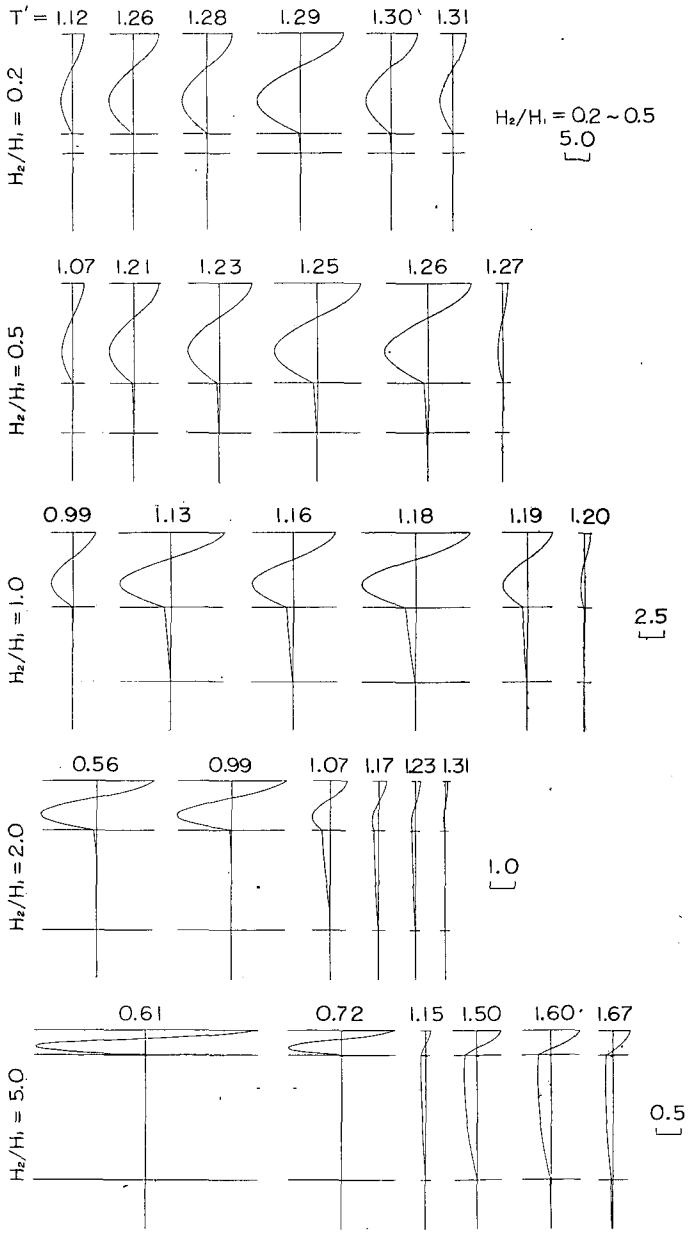

Fig 11 (b). $\mathbf{L_1}$

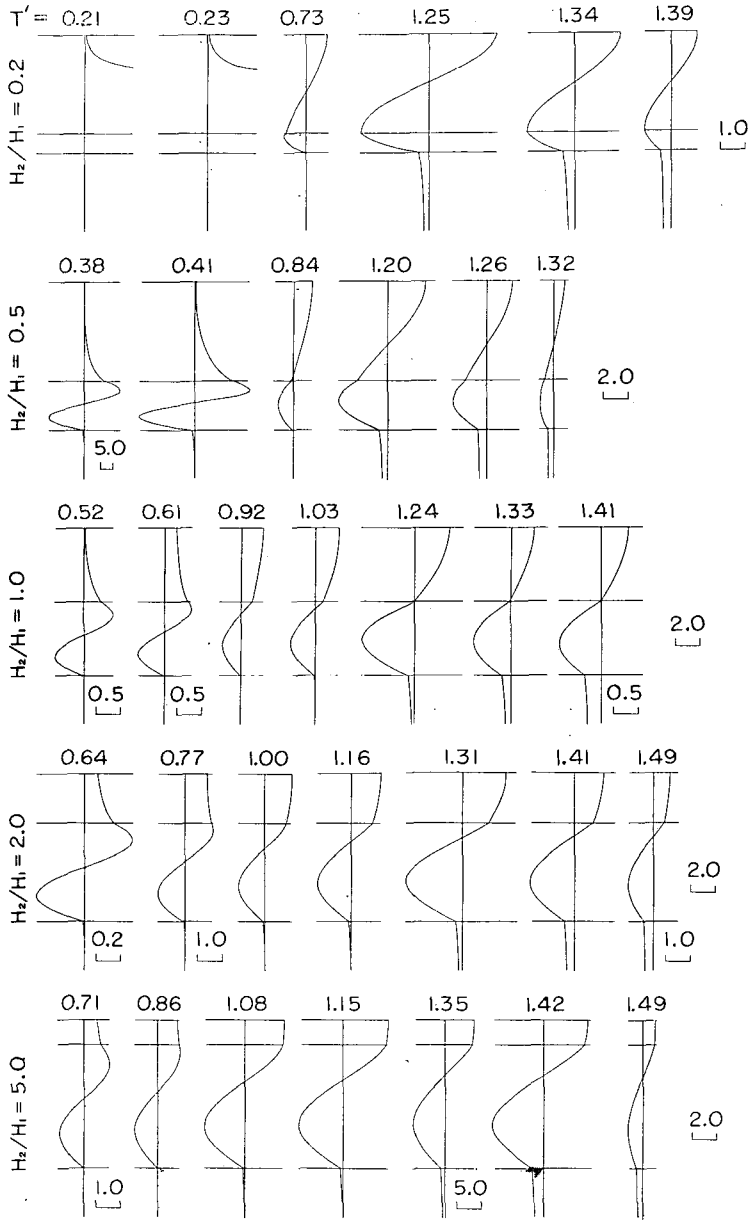

Fig. 11 (c). $\mathbf{L}_1$

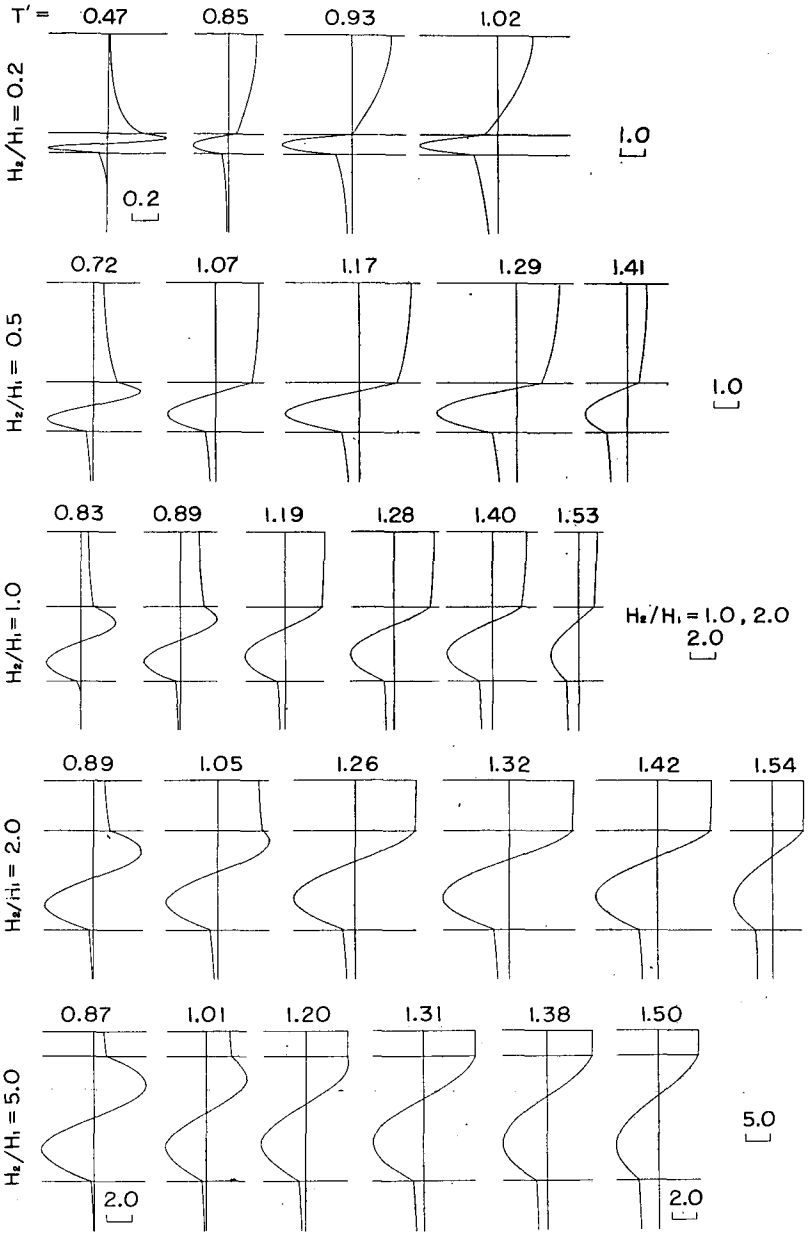

Fig. 11 (d) $\mathbf{L}_1$

Fig. 11. Amplitude distributions for $\mathbf{L}_1$ in cases (A) and (B). $T' = T/(H_1/v_1 + H_2/v_2)$.

indicated by $T'=T/(H_1/v_1+H_2/v_2)$.

Nodes are seen, in Figs. 11(a) and 11(b), in the most superficial layer for all periods. On the other hand in Figs. 11(c) and 11(d), the nodes migrate upwards in the low velocity layer and go into the upper layer with increasing periods.

Actual amplitude distribution does not always show handsome configuration forming 3/4 wave-lengths, whereas (64) is satisfied fairly well at the maximum of the amplitude function.

16. Numerical calculations of the dispersion curve for L_0 and L_1 in cases (C) and (D)

Case (C) from (57) may take the type (iii) in (26). The dispersion curve has been calculated by the characteristic equation (iii) in (27).

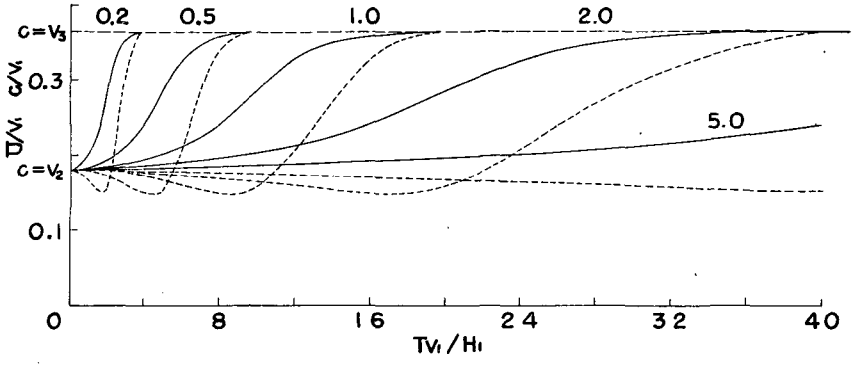

Fig. 12 (a). L_0

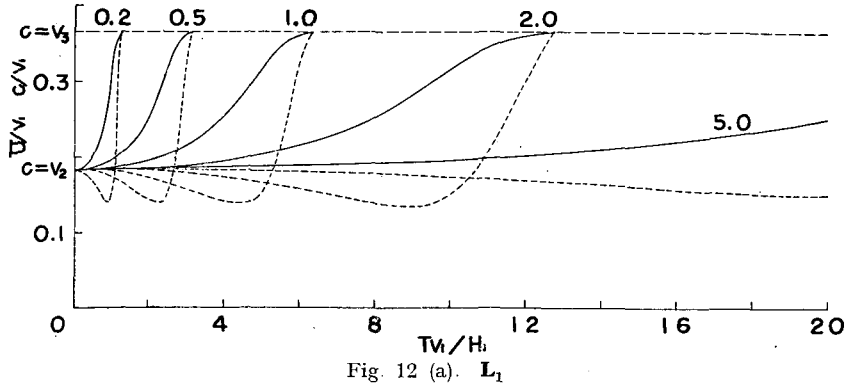

Fig. 12 (a). L_1

Fig. 12 illustrates the first two modes, $\mathbf{L}_0$ and $\mathbf{L}_1$, in the two cases (a) $\mu_2/\mu_1=1/30$, $\mu_3/\mu_2=4$ and (b) $\mu_2/\mu_1=1/30$, $\mu_3/\mu_2=10$, the parameter being H_2/H_1.

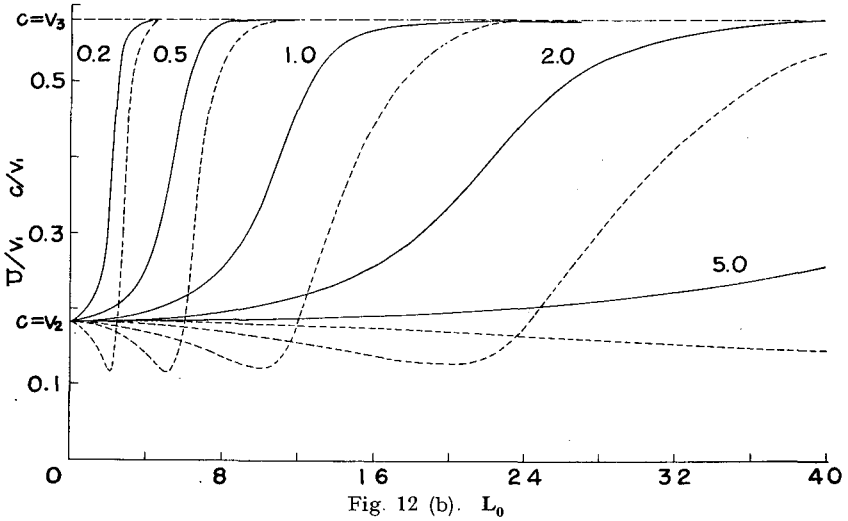

Fig. 12 (b). $\mathbf{L}_0$

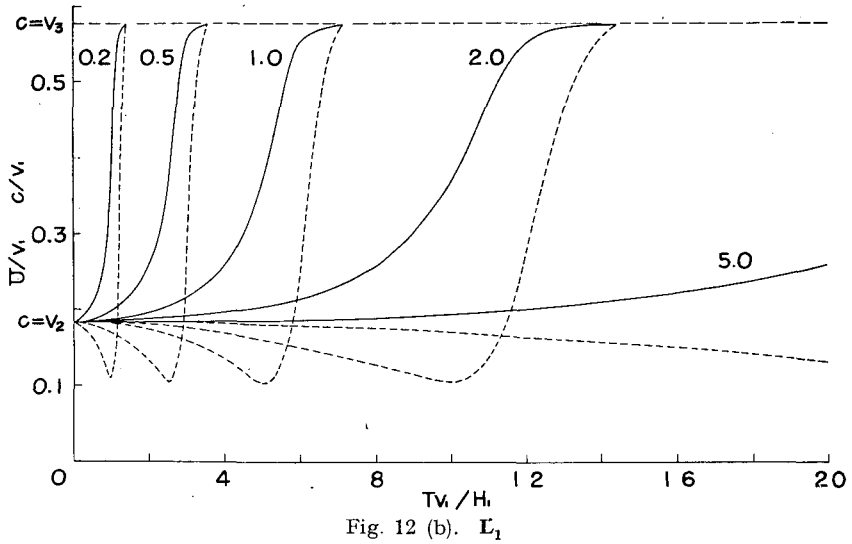

Fig. 12 (b). $\mathbf{L}_1$

Fig. 12. Dispersion curves for $\mathbf{L}_0$ and $\mathbf{L}_1$ in cases (C).
(a) $\mu_2/\mu_1 = 1/30$ aud $\mu_3/\mu_2 = 4$, (b) $\mu_2/_1 = 1/30$ and $\mu_3/\mu_2 = 10$.

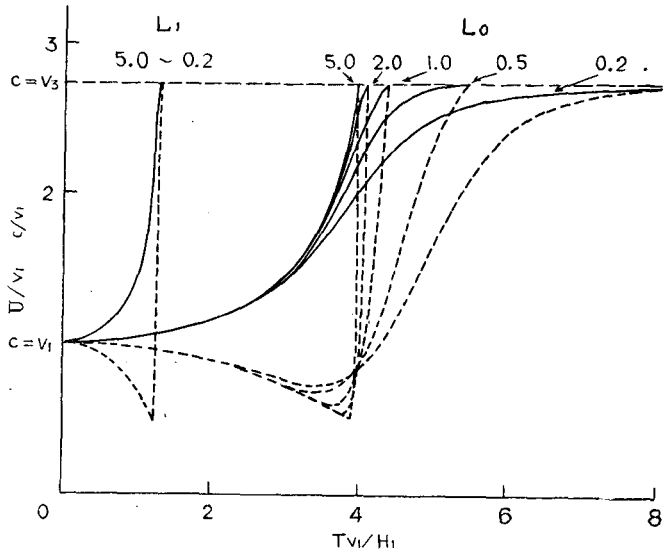

Fig. 13 (a). $\mathbf{L}_0$, $\mathbf{L}_1$

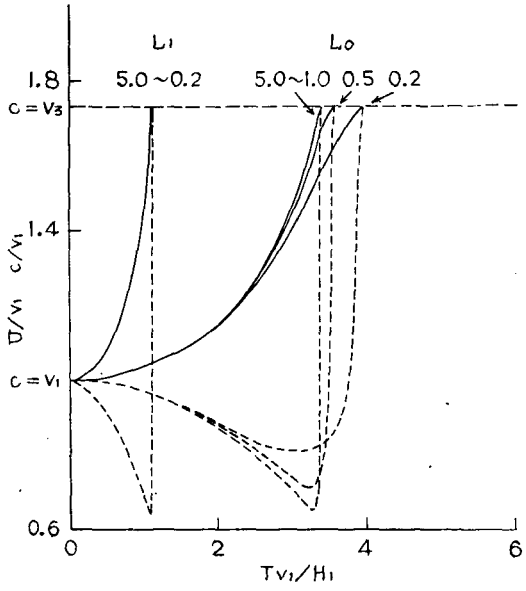

Fig. 13 (b). $\mathbf{L}_0$, $\mathbf{L}_1$

Fig. 13. Dispersion curves for $\mathbf{L}_0$ and $\mathbf{L}_1$ in case (D).
(a) $\mu_2/\mu_1 = 30$ and $\mu_3/\mu_2 = 1/4$, (b) $\mu_2/\mu_1 = 30$ and $\mu_3/\mu_2 = 1/10$.

Case (D) from (57) may take the type (i) in (26). The dispersion curve has been calculated by the characteristic equation (i) in (27). Fig. 13 illustrates the first two modes in the two cases (a) $\mu_2/\mu_1=30$, $\mu_3/\mu_2=1/4$ and (b) $\mu_2/\mu_1=30$, $\mu_3/\mu_2=1/10$, the parameter being H_2/H_1.

In cases (A) and (B), $\mathbf{L}_0$ has no cutoff period. On the other hand in cases (C) and (D), $\mathbf{L}_0$ as well as $\mathbf{L}_1$ has the cutoff period at which phase- and group-velocities coincide respectively with the velocity of S-wave in the lowest layer. The cutoff period must be decreased by increasing the value of H_2/H_1.

In cases (C) and (D) the dispersion curve has only one group velocity minimum, whereas in cases (A) and (B) the curve has two group velocities minimum.

17. Numerical calculations of the amplitude function for $\mathbf{L}_0$ and $\mathbf{L}_1$ in cases (C) and (D)

The results are illustrated in Figs. 14 and 15. The maximum value of

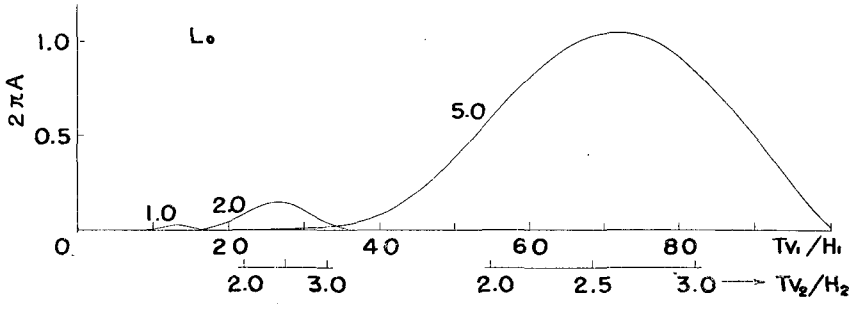

Fig. 14 (a). $\mathbf{L}_0$

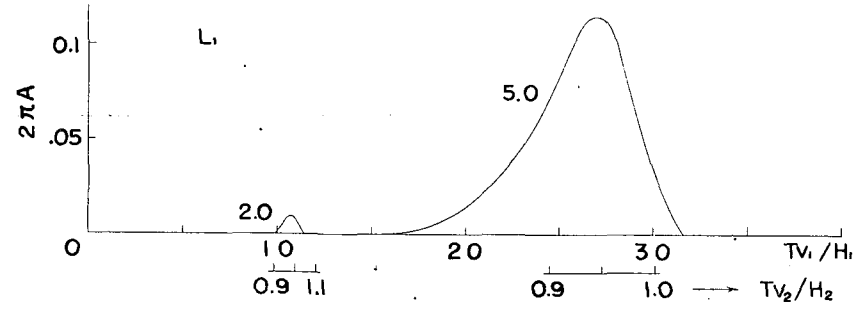

Fig. 14 (a). $\mathbf{L}_1$

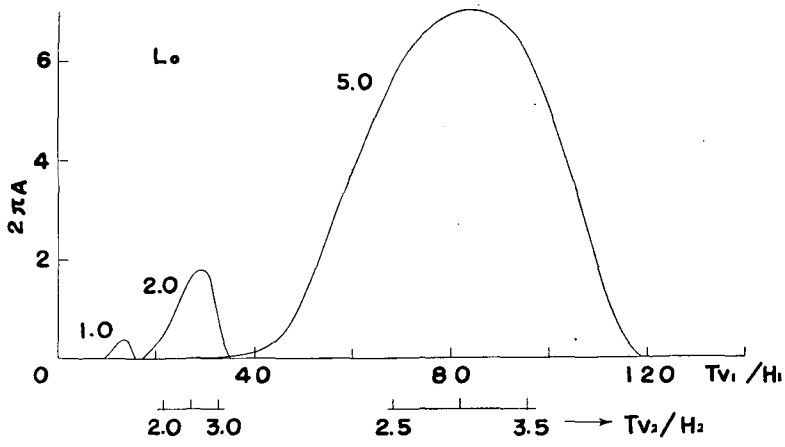

Fig. 14 (b). $\mathbf{L}_0$

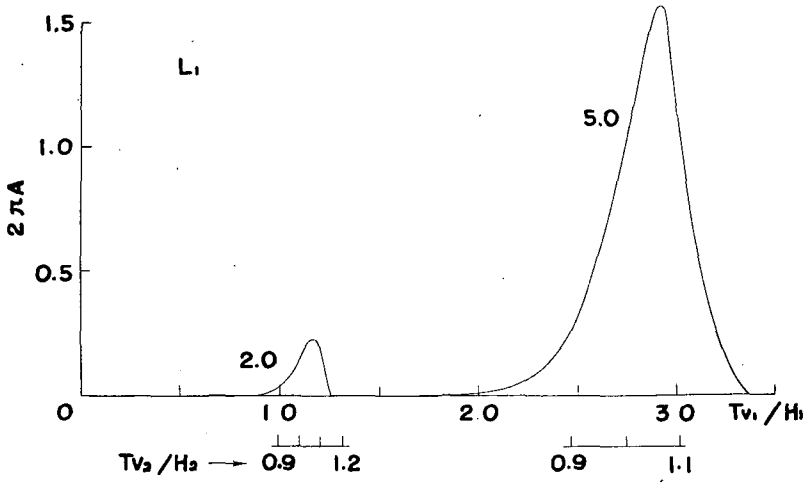

Fig. 14 (b). $\mathbf{L}_1$

Fig. 14. Amplitude functions for $\mathbf{L}_0$ and $\mathbf{L}_1$ in case (C).

the amplitude function is slight when H_2/H_1 is small. However the maximum value increases suddenly with increase of H_2/H_1.

In case (D) the amplitude function for $\mathbf{L}_0$, as shown in Fig. 15, has the maximum near $Tv_1/H_1=4$ and that for $\mathbf{L}_1$ near $Tv_1/H_1=4/3$.

It may be curious that the amplitude function for $\mathbf{L}_1$ in case (D) is not influenced by the ratio H_2/H_1.

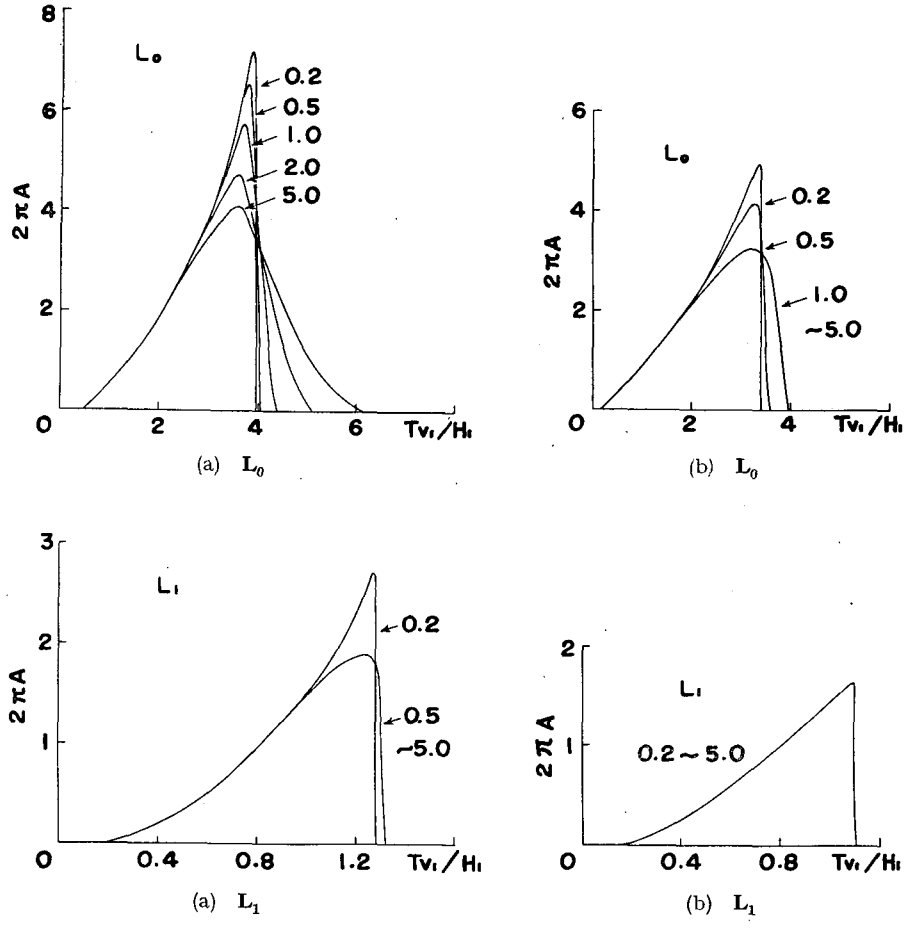

Fig. 15. Amplitude functions for $\mathbf{L}_0$ and $\mathbf{L}_1$ in case (D).

18. Numerical calculations of the amplitude distribution for $\mathbf{L}_0$ and $\mathbf{L}_1$ in cases (C) and (D)

The results are exhibited in Figs. 16 and 17 for several periods indicated by $T/(H_2/v_2)$ or $T/(H_1/v_1)$ respectively.

The amplitude distribution in case (C) may form a type of half wave -length within the second layer, whereas that in case (D) may form a type of quarter wave-length in the first layer.

It must be noted in case (D) that the amplitude in the lowest layer becomes remarkably small, if μ_3/μ_2 decreases or if H_2/H_1 increases.

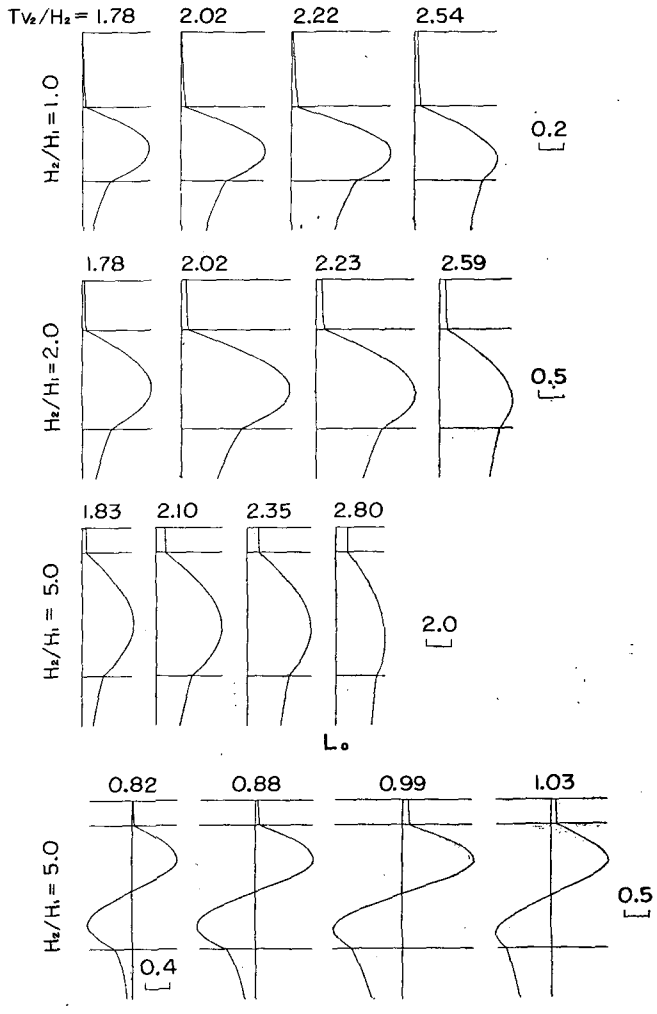

Fig. 16 (a). $\mathbf{L}_0$, $\mathbf{L}_1$

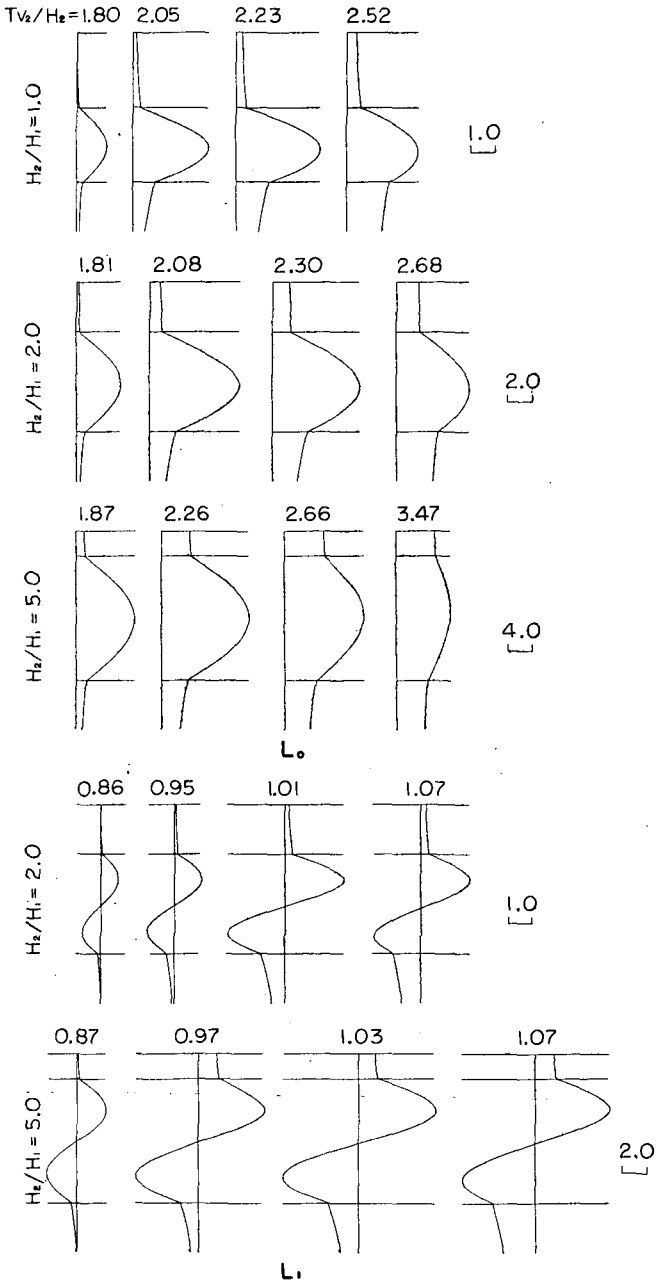

Fig. 16 (b). $\mathbf{L}_0$, $\mathbf{L}_1$

Fig. 16. Amplitude distributions for $\mathbf{L}_0$ and $\mathbf{L}_1$ in case (C).

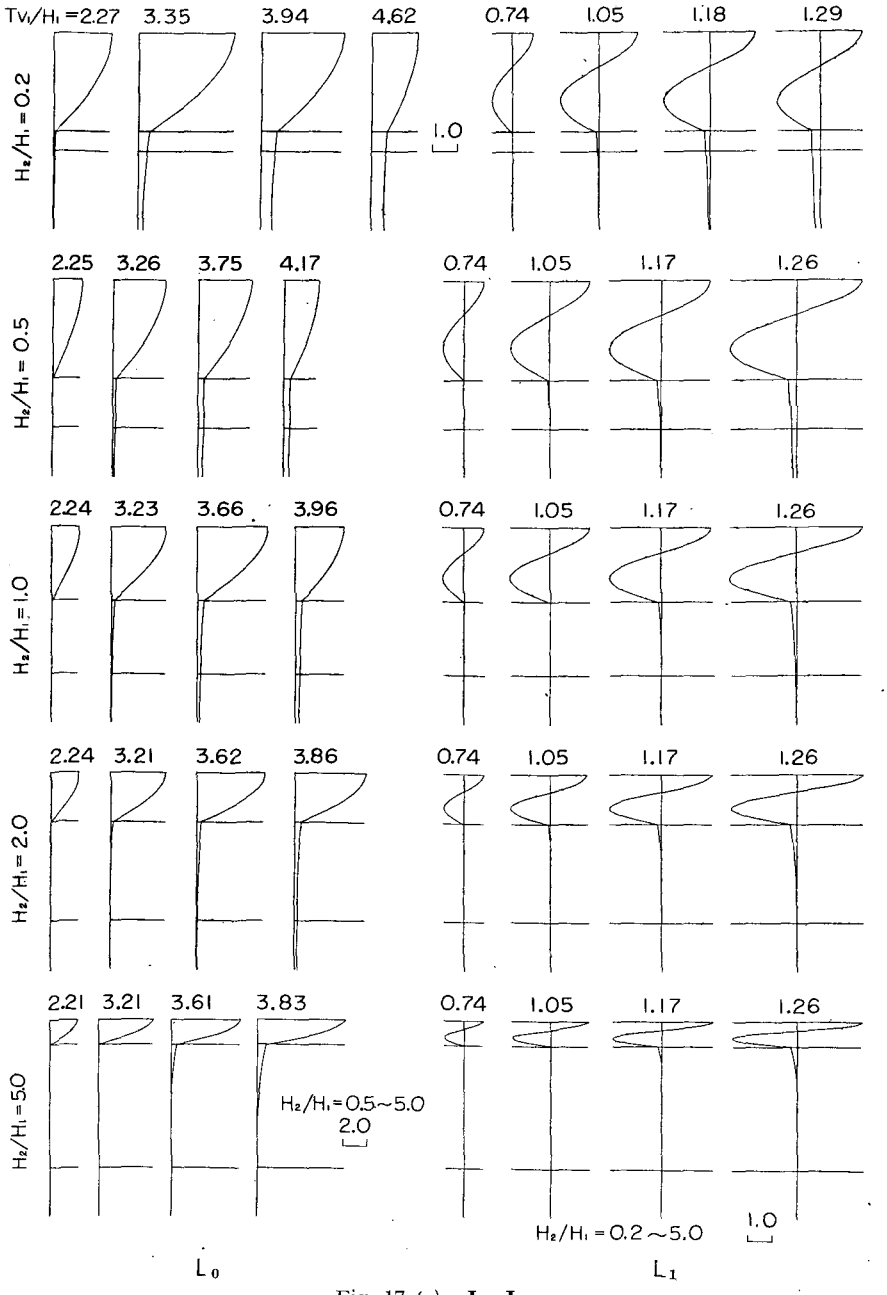

Fig. 17 (a). $\mathbf{L_0}$, $\mathbf{L_1}$

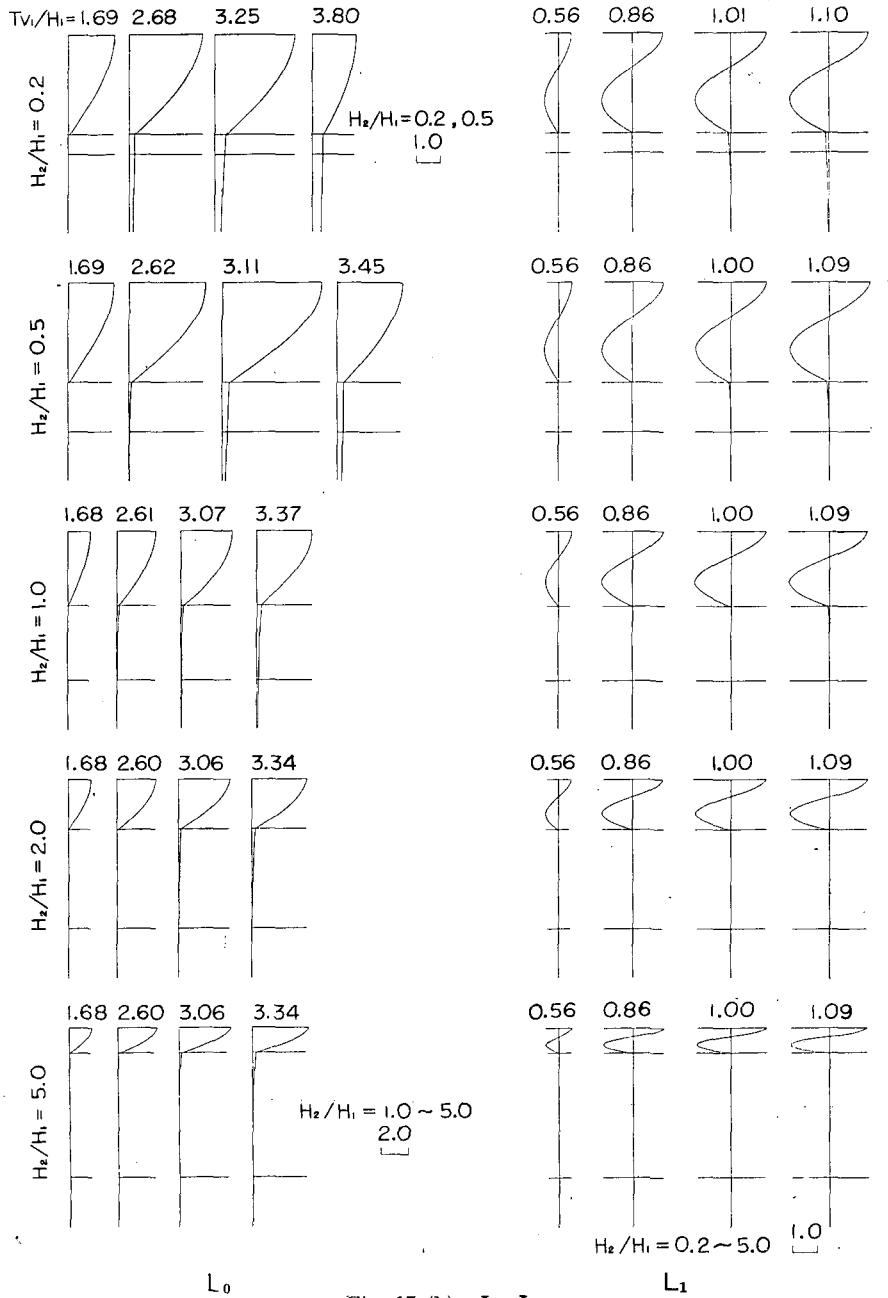

Fig. 17 (b). $\mathbf{L}_0$, $\mathbf{L}_1$

Fig. 17. Amplitude distributions for $\mathbf{L}_0$ and $\mathbf{L}_1$ in case (D).

19. Conclusions

It is the principal aim of this paper to investigate the basic property of LOVE-waves. In order to make the idea concrete, rather large rigidity ratios are assumed in the numerical calculation, regardless of actual conditions of the earth. These large rigidity ratios will be found only near the surface of the earth in seismic prospecting.

"Quarter wave-length law" has been often experienced in actual observations[7)8)]. It has been expected physically that the amplitude of displacement would be large at the phase corresponding to the minimum group velocity. However this expection was too abstract to be connected with that law actually experienced.

If a pulse is generated from a source, the observed displacement must have the factor $\{|dU/d\omega|\}^{-1/2}$, as is well known theoretically[9)10)]. Indeed the displacement of the stationary phase of group velocity will be large, owing to this factor. But the contribution of this facter is not so effective in making the amplitude of the stationary phase larger than that of the other phase.

The present authors have noticed the amplitude function $2\pi A(\xi)$ itself at periodic motion. They have found that the law of (64) was satisfied by the phase corresponding to the maximum of the amplitude function. Due to the factor $(v_1/U-v_1/c)$ contained in $2\pi A(\xi)$, it will be recognized moreover that the minimum group velocity may give the maximum amplitude.

(64) recalls to our minds the vibration of sound in a tube, one end closed. But it was obscure, with this analogy alone, why the period corresponding to the minimum group velocity would satisfy (64). To tell the truth, a quarter wave-length in z-direction is shown by the amplitude distribution more completely at $Tv_1/H_1 \fallingdotseq 0$ than at $Tv_1/H_1 \fallingdotseq 4$. It must be remarked here that the true wave-length in z-direction is $2\pi/\bar{\eta}_1$ and Tv_1 means nothing but an apparent wave-length.

In spite of this physical uncertainty, the acuthors think, the calculated result (64) must be interesting. The observed experience and the abstract consideration, mentioned at the beginning of this section, have been connected well by (64) to each other at least numerically.

In some cases the maximum of the amplitude function is got also near the phase corresponding to the maximum group velocity. This phenomenon is physically less clear than that described already. The low velocity layer must play a grand role in it.

Shielding effect "Quarter wave-length law" is apt to be satisfied by the large

velocity contrast between layers. The nearer the surface of the earth the boundary exists, the larger becomes its effect. If $\mu_2/\mu_1=\mu_3/\mu_2$, for instance, the third layer cannot play an important role but the second layer plays the greatest part. This phenomenon may be recognized by comparison of Fig. 6 (a) with Fig. 6 (b). In Fig. 6 (b) very small energies penetrate into even the second layer. In this circumstance the boundary between the first and the second layers acts as if it were a shielding screen for the lower layers.

In Fig. 6 (a) the subsurface has two screens; one is the boundary between the first and the second layers and the other is that between the second and the third layers. The latter screen is more effective than the former in Fig. 6 (a). Of course, the thicker the layer acting as a screen, the stronger the shielding effect.

Owing to the shielding effect, it will be easy to deduce, by the observation of surface waves, the geological construction near the surface of the earth. On the other hand, deep constructions cannot be deduced from the observation of surface waves, because deep layers must be masked by shallow layers.

Surface waves generated near the surface must be mainly affected by very small constructions near the surface and they will take nearly whole parts of "noise" on the ground.

If the source of the wave lies deep from the surface, only the waves having large wave-length must be taken into account, because the waves having short wave-length have slight amplitude on the ground in this case. This may be understood by Fig. 6, recalling "reciprocal theorem"[1]. LOVE-waves having as large wave-length as the thickness of the earth's crust have been observed in natural earthquakes[8]. Natural earthquakes have so deep sources that the surface waves having short wave-length which might be affected by small construction near the surface cannot be observed on the ground, no matter how large a velocity contrast exists near the surface of the earth.

Now we will conclude that the first boundary which has a large velocity contrast under the source plays the most important role in growth of LOVE -waves. To say it in other words, that first boundary alone will be found by the observation of LOVE-waves.

Acknowledgment The present authors express their thanks to Miss Miyako MUROTA for her help in numerical calculations. The authors wish again to express their thanks to the Ministry of Education for a grant from the Science Research Fund 1958 by the aid of which the present paper has been published.

References

6) TAZIME, K. and OKADA, H.: LOVE-waves in Stratified Three Layers. Journ. Fac. Sci. Hokkaido Univ., Ser. VII, **1** (1958), 115–138.

7) TAZIME, K. and OKADA, H.: Observation of the Velocity of S-waves near the Surface of the Earth. (In Japanese). Butsuri-tanko, **11** (1958), 65–70.

8) STONELEY, R.: Surface Waves Associated with 20° Discontinuity. M. N. R. A. S. Geophys. Suppl., **4** (1937), 39–43.
SEZAWA, K. and KANAI, K.: Relation between the Thickness of a Surface Layer and the Amplitudes of LOVE-waves. Bull. Earthq. Res. Inst., **15** (1937), 577–581.

9) JEFFREYS, H.: Operational Method in Mathematical Physics. C.U.P. (1931), 92–94.

10) PEKERIS, C.L.: Theory of Propagation of Explosive Sound in Shallow Water. Geol. Soc. Am., Mem. **27** (1948).

Errata to the previous paper[6)]

Page	Line or expression		
121	(27) (iii)	$\tanh \hat{\eta}_1 H_1 = \tan \bar{\delta}_{12}$	read $\tanh \hat{\eta}_1 H_1 = -\tan \bar{\delta}_{12}$....
121	last	.... $\coth \left\{\bar{\eta}_1 H_1 \left(\frac{\hat{\eta}_2 H_2}{\bar{\eta}_1 H_1}\right) + \hat{\delta}_{22}'\right\}$	" .... $\coth \left\{\bar{\eta}_1 H_1 \left(\frac{\hat{\eta}_2 H_2}{\bar{\eta}_1 H_1}\right) + \hat{\delta}_{23}'\right\}$
122	(31)	$K_{12} K_{23} - 2i\eta_2 H_2$	" $K_{12} K_{23} e^{-2i\eta_2 H_2}$
125	16	$\cosh (\hat{\eta}_2 H_2 + \hat{\delta}_{23})$	" $\cosh 2 (\hat{\eta}_2 H_2 + \hat{\delta}_{23})$
126	(48)	$\cot \eta_1 H_1 = \frac{\mu_1 \eta_1}{\mu_3 \eta_3} + \ldots.$	" $\cot \eta_1 H_1 = \frac{\mu_1 \eta_1}{i \mu_3 \eta_3} + \ldots.$
127	5∼8	It is very easy to .... of Love-waves.	transfer to below line 5 of page 128
127	15	$2\pi A(\xi) = \omega \left(\frac{1}{U} - \frac{1}{c}\right) \cdot \beta'$	read $2\pi A(\xi) = 2\pi\omega \left(\frac{1}{U} - \frac{1}{c}\right) \cdot \beta'$
127	(52)	$2\pi A(\xi) = \left(\frac{1}{U} - \frac{1}{c}\right)....$	" $2\pi A(\xi) = 2\pi \left(\frac{1}{U} - \frac{1}{c}\right)....$
127	23∼25	It is very easy to .... for $c = v_3$.	transfer to below line 9 of page 128
129	Fig. 2.(C)	Ordinate 2.0	read 1.5
129	6	$T (v_1/H_1 + v_2/H_2) = 4$	" $T/(H_1/v_1 + H_2/v_2) = 4$
138	5	$R_{1,2}$	" $\mathcal{R}_{1,2}^{(1)}$